Electro-Deposited Polycrystalline Gallium Antimonide Films with Stoichiometric Composition

S. Das[1], S. Hussain[2], R. Bhar[3], A. K. Pal[4]
[1, 2, 3, 4] Department of Instrumentation Science
[1, 3, 4] Jadavpur University, Calcutta-700 032, India
[2] UGC-DAE CSR, Kalpakkam Node, Kokilamedu-603104, India

Abstract- *Growth of polycrystalline GaSb thin films by electro-deposition technique with stoichiometric composition is presented in this study. Effect of rapid thermal annealing on the grain size and texture of the resultant films were examined. The films annealed at ~ 673 K, ~ 773 K and ~873 K showed predominantly cubic structure. Band gap values varied between 0.59-0.72 eV for films annealed at different temperatures. X-ray photoelectron spectroscopy (XPS) studies indicated peaks related to Ga and Sb only. Ga–Sb bond was located at ~1117.4 eV. Raman studies indicated peaks located at ~225 cm-1 and ~236 cm-1 representing the LO and TO mode of GaSb, respectively.*

Keywords- GaSb thin films, electro-deposition, XPS, Raman spectroscopy.

I. INTRODUCTION

GaSb, with a direct band gap ~0.7 eV matching well with the 1.55 μm window of silica fibers forms the basis of several optoelectronic devices and the photo detectors operating in the infra-red region. Among the various synthesis routes, electrochemical synthesis of these materials would possibly be an alternative viable low cost technique for depositing these materials in thin film form [1, 2]. Due to its conducive lattice parameter ~0.609 nm similar to that of other semiconductors like InAs, GaAlAs, and CdTe, it can also act as a very good substrate for semiconductor integrated devices [3]. Despite current reports of the poor performance of GaSb based thermophotovoltaic (TPV) cells either in its bulk or in thin-film configurations, applications of GaSb in TPV cells is still a promising challenge [4]. In comparison to the physical vapour deposition and chemical vapour deposition techniques for preparing GaSb films [5, 6], reports of utilizing electrodeposition technique for the synthesis of GaSb films are very few. One of the earlier reports worth citing on deposition of GaSb by electrochemical route was by Paolucci et al. [7]. They indicated reservation against cathodic co-deposition from aqueous media as a viable inexpensive method for the preparation of thin films of binary semiconductors. At this juncture it may be prudent to note that Paolucci et al. indicated that success of the codeposition process could be ascribed to a process in which the rates of electrodeposition of the components were comparable to each other. But the standard potentials of the component elements are generally much different leading to the simultaneous discharge of two or more ions difficult to achieve. They also indicated that matching of the standard potentials might not be an absolute requirement. It was also indicated that besides the above, other factors such as ion activity in solution, over potential at the cathode, presence of complexing agents and/or surfactants, activity of the metals in the alloy might also modulate the ion transfer in the electrolyte. Major issue was to incorporate one ion each of Ga3+ and Sb3+ per unit area per unit time during electrodeposition to make codeposition process a success. Synthesis of GaSb thin films, using a method involving one-step potentiostatic electrodeposition followed by thermal annealing was reported by Yu-Lin et al. [8]. They critically studied the effect of addition of ethylene glycol in aqueous electrolyte solution and discussed the modulation of crystallinity and morphology of the thin films prepared by them. McChesney et al. [9] presented synthesis methods for obtaining GaSb and InSb. The resultant deposit was an admixture of GaSb and Sb. Appearance of such admixtures was ascribed to the control of stoichiometry by the concurrent evolution of H2 and SbH3.

A successful attempt of synthesizing GaSb in polycrystalline form by electrodeposition technique is presented here. Optical, microstructural and compositional properties were studied systematically. Variation of stress and bonding environment for the as-deposited and annealed films are also documented.

II. EXPERIMENTAL

Electrodeposition technique was adopted in this study to deposit GaSb films with stoichiometric composition. The films were deposited onto fluorine doped SnO2 coated glass (40 Ω/□) substrates. The electrolyte was a mixture of 0.04 mol 1-l gallium chloride ($GaCl_3$), 0.002 mol 1-l antimony chloride ($SbCl_3$) and deionized water. The chemicals used here were purchased from Aldrich Chem. Co. and were of 4N grade or higher. Metallic gallium electrode was formed by amalgamating Ga on F-doped SnO_2-coated glass substrate (4 cm long and 1.25 cm width) which served as the counter

electrode (anode). The distance between the cathode (SnO_2 coated glass) and anode surfaces was ~0.8 cm. A dc regulated voltage power supply capable of generating stabilized voltage (0-30 V; 2 A) was used. The deposition was performed at 275 K for 15 min duration with 2 V operating voltage.

A field emission scanning electron microscope (FESEM) (Carl Zeiss SUPRA® 55 with GEMINI® Technology having a resolution ~0.8 nm @ 15 kV) was utilized to carry out surface morphology studies. A Nicolet (MAGNA-IR-750) spectrometer was utilized to record the fourrier transformed infra-red (FTIR) spectra of the films. Transmittance spectra were recorded at room temperature in the wavelength region λ=300-2500 nm by using a spectrophotometer with a photometric accuracy of $\pm$ 0.3%. Micro-structural information was obtained by using a RigakuMiniFlex XRD machine. Photoelectron Spectroscopy (XPS) measurements were carried out using a M/s SPECS make (Germany) spectrometer with a delay line detector. Al Kα was used as the X-ray source at 1486.74 eV. The anode was operated at a voltage of 13kV and source power level was set to 300 W. An Ar ion source was also provided for sputter-etch cleaning of specimens. It was operated at 5kV and 50 μA. The system sputters approximately at the rate of 10 angstroms per minute. This value varies depending on the sample. Spectra were collected using the PHOIBOS 150 HSA analyzer with a resolution of 0.6 eV for 656 kcps at a pass energy of 12 eV. The system was calibrated using standard gold sample. Adventitious carbon peak was used to calculate the peak shifts. Raman spectra were recorded by using a Renishaw inVia micro-Raman spectrometer. Argon laser using 514 nm was used to record the spectra.

III. RESULTS AND DISCUSSION

The key issue of depositing GaSb by electrodeposition technique with assured stoichiometric composition is to adjust the molar concentration of GaCl3 and SbCl3 such that the cathode surface would experience incorporation of one ion each of Ga3+ and Sb3+ per unit area per unit time.

3.1. Microstructural studies

3.1.1. FESEM studies

FESEM micrographs of a representative GaSb film deposited at 275 K for a fixed duration of 15 min on SnO2-coated glass substrates is shown in Fig.1a. It may be observed that the film contained grains with assorted sizes. The as-deposited films were then subjected to rapid thermal annealing (RTA) at three different temperatures (673K, 773K and 873K) keeping the annealing time invariant at 5 min. RTA was performed in argon (99.995%) ambience (~10-2 Torr). The textures of the resultant films are shown in Figs.1(b-d). Change in the surface texture of the GaSb films annealed at different annealing temperatures is apparent from Fig.1b-d. It may be observed that the grain sizes increased with increased annealing temperature and the grain growth was initiated by coalescence of the adjacent grains due to increased adatom mobility. The histograms for all the films are shown in the insets of Fig.1. The grain size distribution curve (inset of Fig.1b) now shows a narrower distribution for films annealed at 673 K compared to that for the film deposited at 275 K (Fig.1a). Higher annealing temperatures made the films more compact as is evident from the FESEM pictures shown in Fig.1c and Fig.1d.

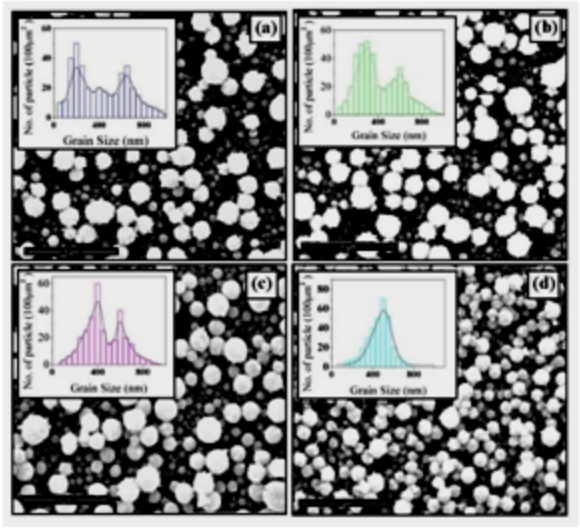

Figure.1. FESEM pictures of GaSb films: (a) as deposited, (b) annealed at 673 K for 5 min, (c) annealed at 773 K for 5 min and (d) annealed at 873 K for 5 min. Insets show the corresponding histograms.

Increase in grain size with narrower grain size distribution could be observed for films annealed at temperatures greater than 673 K conforming grain growth due to coalescence of the adjacent grains due to increased adatom mobility. Films annealed at 873 K indicated faceted grains with narrow grain size distribution curve than that for all films deposited here. EDAX studies indicated that as-deposited films were Sb rich and the films became nearly stoichiometric when

Table-I: Different parameters of GaSb films as deposited and after annealing at different temperature.

Sample	Ga:Sb From EDAX	Crystallite size (nm) (from XRD)	E_g (eV)	ε_α	ω_p ($\times 10^{14}$ s^{-1})	Strain (10^{-4})
GaSb as deposited	0.90	15	0.7	2.78	8.5	9.5
GaSb-673K	0.96	23	0.59	3.09	6.2	4.7
GaSb-773K	0.98	35	0.72	3.40	6.5	8.3
GaSb-873K	1.01	15	0.63	3.24	6.2	1.3

annealed at ~873 K beyond which antimony loss was observed while performing RTA at partial argon pressure. Ga/Sb ratio varied between 0.90 and 1.01 (Table-I).

3.1.2. XRD studies

The XRD traces for the above GaSb films are shown in Fig.2a which indicated that all the GaSb films studied here are polycrystalline with broad grain distribution. The as-deposited films (curve-i) indicated low intensity characteristic peaks of GaSb. However, upon annealing at subsequently higher temperatures, the peak intensities became stronger. The films annealed at ~ 673 K (curve-ii), ~ 773 K (curve-iii) and ~873 K (curve-iv) had predominantly cubic structure with peaks appearing at 2θ~ 26.59°, 30.97°, 37.84°, 51.58°, 54.61°, 65.62°

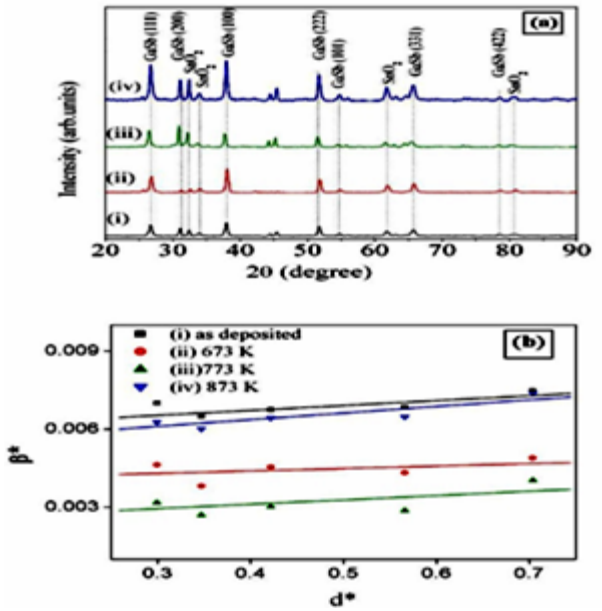

Fig.2. (a) XRD traces: (Curve-i) as-deposited GaSb film. Same film annealed for a fixed time of 5 min at: (Curve-ii) 673K, (Curve-iii) 773 K and (Curve-iv) 873K. (b) Plots of β* versus d*

and 78.34° for reflections from (111), (200), (100), (222), (101), (331) and 422) planes, respectively of cubic GaSb. The peaks originating from reflections from (111) and (100) planes are the most intense ones. These values matched well with those computed by using the experimentally obtained lattice constant. Annealing at higher temperature and at lower partial argon pressure (~10^{-2} Torr) resulted in an increase in the adatom mobility which in turn facilitated growth in the crystallite size. The annealing temperature could not be raised beyond 900 K which resulted in preferential Sb loss as the melting temperature for antimony (which also sublimes) is around ~903 K. This would restrain incorporation of Sb in the GaSb lattice, essential to maintain stoichiometry of the deposited films. Sb loss during annealing at higher temperatures was also indicated by Peccerillo et al [10] and Colombara et al. [11] which was prevented by increased ambient pressure during annealing. Thus, the improvement in crystallinity of the films without affecting stoichiometry could be achieved when annealed at temperatures upto 873 K. Stable cubic structure dominated all the films. The lattice constant (0.61 nm) were computed from the XRD traces which corresponded well to that reported earlier for bulk GaSb (0.61 nm) with cubic structure [12]. Crystallite size, computed from the peaks, are shown in Table-I. It may be noted that although the EDAX results indicated that as-deposited films were Sb rich, we did not observe any additional antimony peak in XRD traces. This may be due to low concentration level of elemental antimony incorporated in the films which might have been in amorphous and/or nanodispersed forms.

Computed strain values were obtained from the plots of β* versus d* (Fig.2b). The strain values computed as above indicated that the residual strain in the films varied between 1-9x10^{-4} and are shown in Table-I. The details of the above calculations could be obtained from reference B.Ghosh [13]. This near invariance of the strains in the films could be associated with the invariance of the grain size in the domain of the substrate temperature of 673-873 K during annealing.

As the strain in the films annealed at ~873 K is minimal, one may consider 873 K to be the optimal annealing temperature for the synthesis of high quality polycrystalline GaSb films.

3.2 Optical Measurements

Transmission spectra of the GaSb films are shown in Fig.3a. The fall in the transmittance curve near band gap region depended on the annealing temperature. Sharpness of the fall of the absorption edge near band gap region also depended on the crystallinity of the films which in turn depended on the annealing temperature as indicated by the XRD measurement. The absorption coefficient (α) was determined using the method described in the references [14, 15]. The absorption coefficient (α) may be expressed as:

$$\alpha = (A/h\nu)(h\nu - E_g)^m \qquad (1)$$

and hence,

$$\frac{d[\ln(\alpha h\nu)]}{d[h\nu]} = \frac{m}{h\nu - E_g} \qquad (2)$$

where, the constant A is different for different transitions. Different m values would indicate different transitions occurring in the films. E_g is the corresponding band gap. Now, if we plot d[ln(αhν)]/d[hν] versus hν, it should show divergence at hν~E_g. For allowed direct, allowed indirect, forbidden direct and forbidden indirect transitions, m would have values of l/2, 2, 3/2 and 3, respectively. GaSb film is known to have allowed direct (E_g) transitions and as such one clear divergence at E_g~ 0.66eV was noticed in the d[ln(αhν)]/d[hν] versus hν plot at hν~E_g. Now, using the above approximate E_g values, m can be easily computed from the

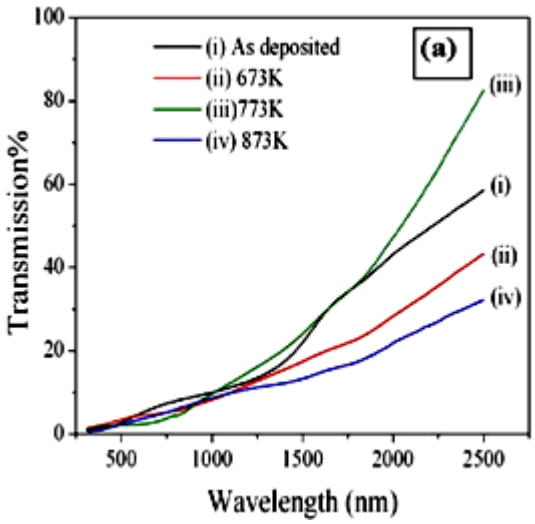

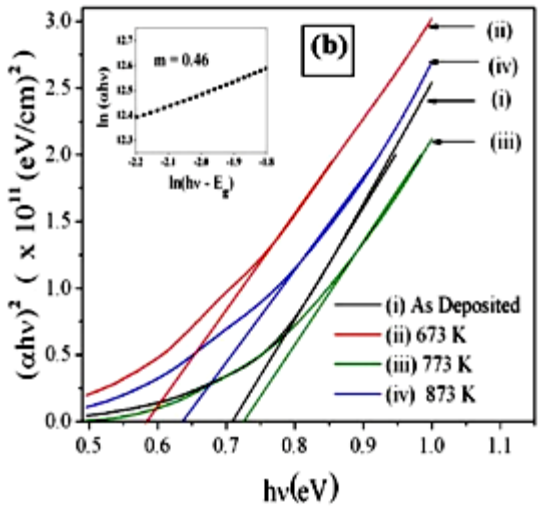

Fig.3. (a) Transmission spectra of the GaSb films and (b) $(\alpha h\nu)^2$ versus hν plots for the GaSb films (inset shows the plots of ln(αhν) versus ln(hν- E_g) of representative film annealed at 773 K): where (i) As Deposited film, (ii) Annealed at 673 K, (iii) annealed at 773 K, (iv) annealed at 873 K.

slopes of ln(αhν) versus ln(hν-E_g) plots (inset of Fig.3b). The values of m obtained for the GaSb films studied here varied between 0.46-0.51. Linear portions of the plots of $(\alpha h\nu)^2$ versus hν were extrapolated to zero to obtain the value of the band gaps. The above plots for the GaSb films studied here are shown in Fig.3b. The values of band gap obtained as above varied between 0.59-0.72 eV (Table I).

Xue et al. [16] presented a modified Kramers-Kronig (KK) theory which was used for evaluating thickness, refractive index and extinction coefficient of the GaSb films studied here. The details of this method for simultaneous computation of the optical parameters of transparent thin film along with its thickness were presented in the publication [17] and the references therein. We have utilized the above modified theory to evaluate the thickness, refractive index and extinction coefficient values of GaSb films studied here.

The as-deposited films are not as dense as those annealed at higher temperatures (Fig.4a). The refractive indices (n) were also found to vary (Fig.4a) from 1.75 to 2.15 within the measured wavelength range of 500-2500 nm for the films deposited in this study. Dependence of the extinction coefficient (k) on the wavelength is also shown in Fig.4a. Similar to the variation of refractive index, extinction coefficient of the as-deposited films was

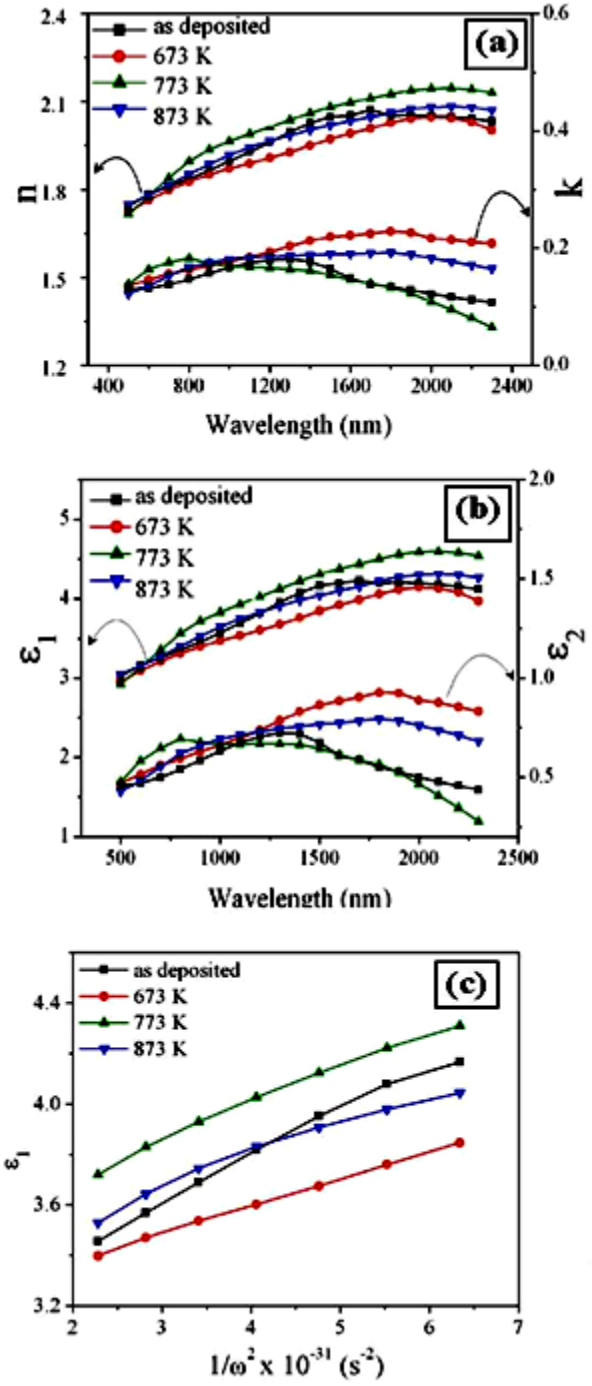

Fig.4. (a) Plots of n versus λ, and k versus λ, (b) plots of ε_1 versus λ, and ε_2 versus λ, (c) plots of ε_1 versus $1/\omega^2$.

higher than those annealed at higher temperatures and all of them increased near the band gap energy. The real part of the dielectric constant (ε_1) and its imaginary part (ε_2) computed as above for all the λ values under consideration in this experiment are shown in Fig.4b. ε_1 and ε_2 values obtained here did not show any regular variance for films annealed at different temperatures. The variation of ε_1 with photon energy depends on the plasma frequency (ω_p) and can be expressed as [18]:

$$\varepsilon_1 = \varepsilon_\infty - (\varepsilon_\infty \omega_p^2)/\omega^2 \qquad (3)$$

Here, the limiting value of the high frequency dielectric constant is ε_∞. Variation of ε_1 with inverse of the square of the frequency ($1/\omega^2$) of incident radiation for all the GaSb films studied here is shown in Fig.4c. The value of ω_p and ε_∞ have been determined from the slope and the intercept of the linear portion of the ε_1 vs. $1/\omega^2$ plots (Fig.4c) and are shown in Table-I. The value of ε_∞ determined as above for the GaSb films varied between 2.7 and 3.4. It may be noted here that Ghosh et al. [19] reported the values of ε_∞ within the range of 3.11 – 5.37. Except for the values of the as-deposited film reported here, ω_p values agreed well with those obtained by Ghosh et al. [19]. The plasma frequency (ω_p) obtained for the annealed films were in the range of 6.2 to 6.5 x 10^{14} s^{-1}.

3.3 XPS studies

It may be prudent to examine the XPS spectra of a representative as-deposited and annealed (at 873 K for 5 min) film to represent the bonding behavior of the GaSb films. The survey spectra of a representative as-deposited GaSb film along with that for films annealed at 873 K are shown in Fig.5a and Fig.5b, respectively. It may be noted that the survey spectra for all the films deposited here were nearly the same with the exception of varying intensities of the peaks for the core level spectra for Ga and Sb. Peaks at ~ 20.9 eV for Ga3d, ~35.0 eV for Sb4d, ~529.4 eV for peaks for $Sb3d_{5/2}$, and ~814.5 eV for $Sb3p_{1/2}$ dominated the survey spectra. The peak for $Ga2p_{1/2}$ appeared at ~1144 eV while that for $Ga2p_{3/2}$ appeared at ~1117 eV. The peak at ~105 eV has originated from the overlapping of peaks for $Ga3p_{1/2}$, $Ga3p_{3/2}$ and Sb4p.

Core level spectra of a representative GaSb film annealed at 873 K for 5 min have been examined critically as this film showed the best crystallinity and topographical behavior. If we now concentrate on the Fig.5c and Fig.5d for the core level spectra of Sb, one may observe (Fig.5d) that the

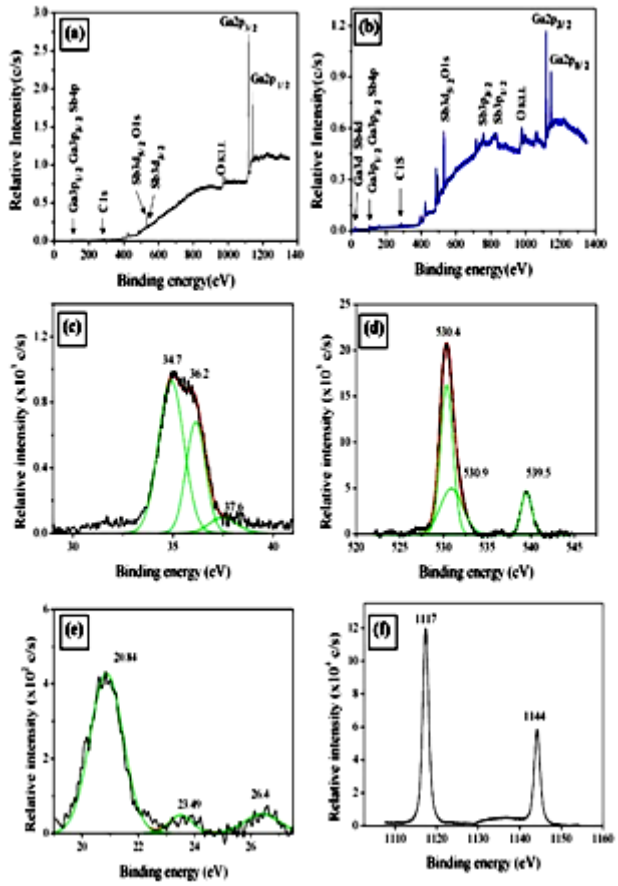

Fig.5. General survey spectra of (a) as deposited GaSb film and (b) film annealed at 873 K. Core level spectra for annealed film: (c) Sb4d, (d) $Sb3d_{5/2}O1s$ $Sb3d_{3/2}$, (e) Ga3d Ga2d Sb4d peak and (f) Ga $2p_{3/2}$ and Ga $2p_{1/2}$ core-level spectra.

core-level spectra for Sb3d consisted of a strong peak at ~530.7 eV associated with a lower intensity peak at ~540.1 eV. The Sb4d spectra (Fig.5c) could be deconvoluted into three components. The peaks located at ~34.7 eV and ~36.2 eV could be ascribed to the spin orbital split peaks of $Sb4d_{3/2}$ and $Sb4d_{5/2}$ for Sb-Ga with a spin–orbit splitting of 1.25 eV. The low intensity third component at ~ 37.6 eV may be an indicative of the presence of oxide in the film. The intensity of this peak suggests that there may not be much of oxide components present in the films. The peak at ~540.1 eV could be attributed to the binding energy of $Sb3d_{3/2}$. One may observe some asymmetry in this peak also. Upon deconvolution, presence of two peaks located at 530.4 eV and 530.9 eV constituting the peak at ~530.7 eV could be observed. The low intensity peak at ~530.9 eV indicates the presence of oxides at a very low concentration level. The other peak at ~530.5 eV could be identified as arising due to the binding energy of $Sb3d_{3/2}$. Morgan et al [20] also observed this peak. It was observed that the relative ratio of the area of the $Sb3d_{3/2}$-$3d_{5/2}$ doublet was slightly smaller (1:2). Peak at 20.84 eV could also be deconvoluted in two peaks (Fig.5e) and they could be attributed to spin-orbital split peaks for $Ga3d_{5/2}$ and $Ga3d_{3/2}$. The two broad low intensity peaks located at ~23.49 and ~26.4eV could be assigned to the oxidized form of the Ga 3d and Sb 4d bands. No signals due to metallic gallium were observed. The Ga–Sb bond located at ~1117.4 eV as in GaSb along with a peak at ~1118.8 eV related to Ga–O bond as in Ga_2O_3 was observed (Fig.5f). The observed Ga $2p_{3/2}$ core-level spectra match well with that for bulk GaSb (1117.5 eV) [21, 22].

3.5. Raman studies

Fig. 6a and Fig6b show the Raman spectrum of the as-deposited GaSb film and that for the same film subjected to rapid thermal annealing at 873 K for 5 min,

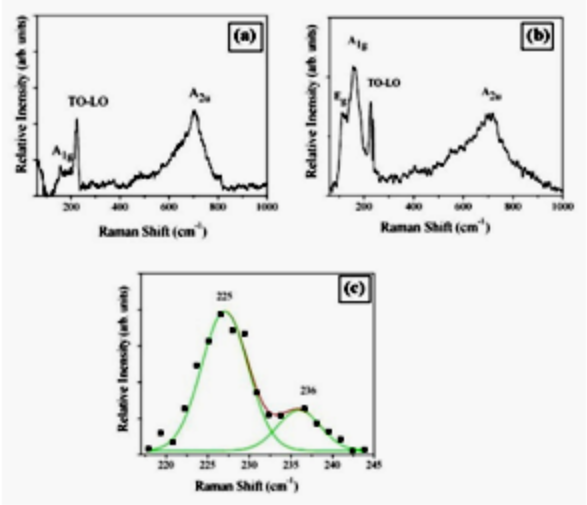

Fig.6 Raman spectra of a representative GaSb film: (a) as-deposited, (b) annealed at 873 K for 5 min and (c) deconvoluted peak for LO and TO mode of GaSb

respectively. A strong peak located at ~226 cm^{-1} dominated the spectra. This peak may be associated with the optical modes at the zone center. This frequency matches well with that observed (~231 cm^{-1}) from neutron scattering measurement [23]. A weak peak at ~157 cm^{-1} due to A_{1g} mode of Sb-Sb bond vibration was also observed [24]. The intensity of both the above peaks increased significantly for the annealed film (Fig.6b). The peak at 226 cm^{-1} could be deconvoluted into two peaks at ~225 cm^{-1} and ~236 cm^{-1} (Fig.6c). These two peaks would represent the LO and TO mode of GaSb, respectively [25]. It may be noted here that only the LO mode is allowed for (100) oriented GaSb material and the TO mode is forbidden [26, 27] and as such the observed intensity of the TO mode is small compared to that for LO mode. Another broad peak observed at ~707 cm^{-1} could be attributed to the A_{2u} LO modes of SnO_2 substrate

[28]. The weak peaks at ~157 cm^{-1} (for as-deposited film) and at 115 cm^{-1} (for annealed film) could be related to the E_g and A_{1g} Sb–Sb bond vibrations, respectively. This observation matches well with the findings of Winnerl et al. [29] who concluded from their studies on GaSb wafers subjected to single thermal treatment that the Raman lines appearing at ~115 cm^{-1} and ~150 cm^{-1} would correspond to E_g and A_{1g} Sb–Sb bond vibrations.

IV. CONCLUSIONS

Electrochemical deposition technique was adopted to deposit polycrystalline gallium antimonide films with stoichiometric composition on SnO_2-coated glass substrates. The deposited films were predominantly of cubic structure with intense reflections from (111), (100) and (222) planes. Residual strain in the films was calculated from the XRD traces and found to be invariant for all the films. The films annealed at ~ 673 K, ~ 773 K and ~873 K showed predominantly cubic structure. Band gap values varied between 0.59-0.72 eV for films annealed at different temperatures. Films became more stoichiometric when annealed at increased annealing temperature. The XPS spectra were dominated by the presence of peaks at ~ 35.0 eV for Sb4d, ~530 eV peaks for $Sb3d_{5/2}$, and ~814.8 eV for $Sb3p_{1/2}$. $Ga2p_{1/2}$ peak appeared at ~1144 eV while that for $Ga2p_{3/2}$ appeared at ~1117 eV. Raman spectra were dominated by a strong peak at ~226 cm^{-1} along with a weak peak at 157 cm^{-1}, corresponding to the optical modes of GaSb and A_{1g} modes of Sb-Sb bond vibration, respectively. XPS and Raman studies indicated the presence of small amount of elemental antimony in the films although XRD traces did not indicate peaks related to elemental Sb. Considering all aspects of the films deposited by the technique described here, it may be concluded that this method is certainly superior to that reported in ref. [9]. This report presents an in depth picture of the structure and composition of the GaSb films synthesized by electro-deposition technique.

ACKNOWLEDGEMENT

The authors wish to thank the UGC-DAE CSR and Board of Research in Nuclear Sciences (BRNS) Government of India for the financial assistance for executing this programme. Fellowship awarded to S.D by the Board of Research in Nuclear Sciences (BRNS), Government of India is acknowledged with thanks.

REFERENCES

[1] K. Premaratne, S.N. Akuranthilaka, I.M. Dharmadasa and A.P. Samantilleka “Electro deposition using non-aqueous solutions at 170 ^oC and characterization of CdS, $CdS_xSe_{(1-x)}$ and CdSe compounds for use in graded band gap solar cells” Renewable Energy, Vol. 29, 2003, pp. 549-557.

[2] S.J. Lade, M.D. Uplane and C.D. Lokhande “Photo electrochemical properties of CdX (X= S, Se, Te) films electrodeposited from aqueous and non-aqueous baths” Mater. Chem. Phys. Vol. 68, 2001, pp. 6–41.

[3] Q. Zaixiang, S. Yun, H. Weiyu, H. Qing and L. Changjian “Polycrystalline GaSb thin films grown by co-evaporation” J. Semicond. Vol. 30, 2009, pp. 033004.

[4] Y.K. Noh, M.D. Kim, J.E. Oh and W.C. Yang “Structural and Optical Properties of GaSb Films Grown on AlSb/Si (100) by Insertion of a Thin GaSb Interlayer Grown at a Low Temperature” J. Korean Phys. Soc. Vol. 57, 2010, pp.173-177.

[5] P. S. Dutta, H. L. Bhat and V. Kumar “The physics and technology of gallium antimonide: An emerging optoelectronic material” J. Appl. Phys. Vol. **81**, 1997, pp. 5821.

[6] C. D. Lokhande, and S. H. Pawar “Electrodeposition of Thin Film Semiconductors” phys. stat. sol. (a), Vol. 111, 1989, pp. 17-40.

[7] F. Paolucci, G. Mengoli and M. M. Musiani “An electrochemical route to GaSb thin films” J. Appl. Electrochemistry, Vol. 20, 1990, pp. 868-873.

[8] X. Yu-lin, P. Yuan-chun, S. A. Bai-sheng, Z. Jian and S. Zhi-mei “Aqueous electrochemical deposition film GaSb phase change” J. Electrochem. Vol. 20, 2014, pp.134-138.

[9] J.J. McChesney, J. Haigh, I.M. Dharmadasa and D.J. Mowthorpe “Electrochemical growth of GaSb and InSb for applications in infra-red detectors and optical communication systems” Optical Materials, Vol. 6, 1996, pp. 63-67.

[10] E. Peccerillo, J. Major, L. Phillips, R. Treharne, T. J. Whittles, V. Dhanak, D. Halliday, and K. Durose “Published in 2014 IEEE 40th Photovoltaic Specialist Conference (PVSC)” Vol. 2014, 2014, pp. 0266-0269.

[11] D. Colombara, L.M. Peter, K. D. Rogers, and K. Hutchings “Thermochemical and kinetic aspects of the

sulfurization of Cu–Sb and Cu–Bi thin films" Journal of Solid State Chemistry, Vol. 186, 2012, pp. 36–46.

[12] Ch. B. Lioutas, G. Zoulis, S. Konidaris, E.K. Polychroniadis, and D. Stro´z "On the structured imperfections of bulk GaSb using high resolution transmission electron microscopy" Micron, Vol. 40, 2009, pp. 6–10.

[13] B. Ghosh, S. Hussain, D. Ghosh, R. Bhar, and A.K. Pal, "Studies on CdTe films deposited by pulsed laser deposition technique" Physica B, Vol. 407, 2012, pp. 4214–4220.

[14] J.C. Manifacier, J. Gasiot, and J.P. Fillard, "A simple method for the determination of the optical constants n, k and the thickness of a weakly absorbing thin film" J. Phys. E, Vol. 9, 1976, pp. 1002-1004.

[15] D. Bhattacharya, S. Chaudhuri, and A.K. Pal "Bandgap and optical transitions in thin films from reflectance measurements" Vacuum, Vol. 43, 1992, pp. 313-316.

[16] S.W. Xue, X.T. Zu, W.G. Zheng, H.X. Deng, and Z. Xiang "Effects of Al doping concentration on optical parameters of ZnO:Al thin films by sol–gel technique" Physica B, Vol. 381, 2006, pp. 209-213.

[17] S.R. Bhattacharyya, R.N. Gayen, R. Paul, and A.K. Pal "Determination of optical constants of thin films from transmittance trace" Thin Solid Films, Vol. 517, 2009, pp. 5530-5536.

[18] J.I. Pankove "Optical Processes in Semiconductors" Prentice-Hall Inc, NJ, USA, 1971, pp-89.

[19] D. Ghosh, B. Ghosh, S. Hussain, R. Bhar, and A. K. Pal "Polycrystalline GaSb films prepared by the coevaporation technique" Appl. Phys. A, Vol. 115, 2014, pp. 1251–1261.

[20] W. E. Morgan, W. J. Stec, and J. R. V. Wazer "Inner-Orbital Binding-Energy Shifts of Antimony and Bismuth Compounds" Inorganic Chemistry Vol. 12, 1973, pp. 953-955.

[21] F. M. Liu, and L. D. Zhang, "X-ray photoelectron spectroscopy of GaSb nanoparticles embedded in SiO2 matrices by radio-frequency magnetron co-sputtering" Semicond. Sci. Technol. Vol. 14, 1999, pp. 710–714.

[22] Z. Y. Liu, T. F. Kuecha, and D. A. Saulys "Improved characteristics for Au/n-GaSb Schottky contacts through the use of a nonaqueous sulfide-based passivation" Appl. Phys. Lett. Vol. 83, 2003, pp. 2587-2589.

[23] B. Rakshit, V. Srivastava, S. P. Sanyal, P. K. Jha, T. R. Ravindran, and A. K. Arora "Vibrational spectroscopy and phonon dispersion of GaSb, Indian" J. of Pure & App. Phys. Vol. 46, 2008, pp. 20-22.

[24] C. E. M. Campos, and P. S. Pizani, "Strain effects on As and Sb segregates immersed in annealed GaAs and GaSb by Raman spectroscopy" J. Appl. Phys., Vol. 89, 2001, pp. 363-3633.

[25] C. E. M. Campos, and P. S. Pizani "Morphological Studies of Annealed GaAs and GaSb surfaces by micro-Raman spectroscopy and EDX microanalysis" Appl. Surf. Sci., Vol. 200, 2002, pp. 111-116.

[26] S. G. Kim, H. Asahi, M. Seta, J. Takizawa, S. Emura, R. K. Soni, and S. Gonda, "Raman scattering study of the recovery process in Ga ion implanted GaSb" J. Appl. Phys., Vol. 74, 1993, pp. 579-585.

[27] Y.K. Su, K.J. Gan, J.S. Hwang, and S.L. Tyan, "Raman spectra of Si implanted GaSb" J. Appl. Phys., Vol. 68, 1990, pp. 5584-5587.

[28] X. S. Peng, L. D. Zhang, G. W. Meng, Y. T. Tian, and Y. Lin "Micro-Raman and infrared properties of SnO2 nanobelts synthesized from Sn and SiO2 powders" J. Appl. Phys. Vol. 93, 2003, pp. 1760-1763.

[29] S. Winnerl, S. Sinning, T. Dekorsy, and M. Helm, "Increased terahertz emission from thermally treated GaSb" Appl. Phys. Lett., Vol. 852004, pp. 3092-3094.